Journal of Colloid and Interface Science 355 (2011) 486–493

Contents lists available at ScienceDirect

Journal of Colloid and Interface Science

www.elsevier.com/locate/jcis

Dielectrophoretic alignment of metal and metal oxide nanowires and nanotubes: A universal set of parameters for bridging prepatterned microelectrodes

A.W. Maijenburg [a], M.G. Maas [a], E.J.B. Rodijk [a], W. Ahmed [b], E.S. Kooij [b], E.T. Carlen [c], D.H.A. Blank [a], J.E. ten Elshof [a,*]

[a] Inorganic Materials Science, MESA+ Institute for Nanotechnology, University of Twente, P.O. Box 217, 7500 AE Enschede, The Netherlands
[b] Physics of Interfaces and Nanomaterials, MESA+ Institute for Nanotechnology, University of Twente, P.O. Box 217, 7500 AE Enschede, The Netherlands
[c] BIOS Lab-on-a-Chip Group, MESA+ Institute for Nanotechnology, University of Twente, P.O. Box 217, 7500 AE Enschede, The Netherlands

ARTICLE INFO

Article history:
Received 13 October 2010
Accepted 3 December 2010
Available online 10 December 2010

Keywords:
Templated electrodeposition
Dielectrophoresis
Alignment
Nanowires
Nanotubes

ABSTRACT

Nanowires and nanotubes were synthesized from metals and metal oxides using templated cathodic electrodeposition. With templated electrodeposition, small structures are electrodeposited using a template that is the inverse of the final desired shape. Dielectrophoresis was used for the alignment of the as-formed nanowires and nanotubes between prepatterned electrodes. For reproducible nanowire alignment, a universal set of dielectrophoresis parameters to align any arbitrary nanowire material was determined. The parameters include peak-to-peak potential and frequency, thickness of the silicon oxide layer, grounding of the silicon substrate, and nature of the solvent medium used. It involves applying a field with a frequency $>10^5$ Hz, an insulating silicon oxide layer with a thickness of 2.5 μm or more, grounding of the underlying silicon substrate, and the use of a solvent medium with a low dielectric constant. In our experiments, we obtained good results by using a peak-to-peak potential of 2.1 V at a frequency of 1.2×10^5 Hz. Furthermore, an indirect alignment technique is proposed that prevents short circuiting of nanowires after contacting both electrodes. After alignment, a considerably lower resistivity was found for ZnO nanowires made by templated electrodeposition ($2.2–3.4 \times 10^{-3}$ Ωm) compared to ZnO nanorods synthesized by electrodeposition (10 Ωm) or molecular beam epitaxy (MBE) (500 Ωm).

1. Introduction

Synthesis of one-dimensional nanostructures, such as nanowires and nanotubes, has attracted increasing attention in the past years. The unique physical and chemical properties of these nanostructures make them promising building blocks for various kinds of future applications, such as nanosensors [1–3], cell trackers [4–6], and self-propelling nanomotors [7–9].

A range of processes has been used for the synthesis of various types of nanowires. They include both vapor-phase techniques and liquid-phase techniques [4,10–13]. As the increasing emphasis on low cost, high throughput, high volume, and ease of production has made template-directed electrodeposition emerge as a promising process, we chose this technique for nanowire synthesis. Template-directed electrodeposition belongs to the group of wet-chemical synthesis techniques and can be carried out at or near room temperature and at ambient pressure. Various types of materials, such as metals, conducting polymers, and semiconductors can be deposited with it. Another advantage of template-directed electrodeposition is the possibility to form nanotubes as well [4,10–13].

A very important and challenging part of the integration of nanowires or nanotubes into functional devices concerns the alignment of nanowires between two or more electrodes. Several techniques for the alignment of nanowires between electrodes have been reported, such as *in situ* micromanipulation [14], focused ion beam deposition [14,15], electron beam lithography [14], drop-casting of wires from a solution onto prepatterned electrodes [14], dielectrophoresis [16–21], and magnetic alignment [10,22–26]. We chose dielectrophoresis as the nanowire alignment technique in the present study, because it can be used under ambient conditions without capital-intensive equipment and can be employed to align all kinds of nanowire materials.

Fig. 1 illustrates the working principles of dielectrophoretic alignment of nanowires between two planar electrodes. Essentially, an alternating electric field is generated between the electrodes that captures the nanowire, and attracts and orients it until it bridges the gap between the electrodes. This process is called positive dielectrophoresis. It requires the dielectric constant of the nanowire material to be higher than the dielectric constant of the surrounding medium. In the case that the dielectric constant of the nanowires is lower than that of the surrounding

* Corresponding author. Fax: +31 53 4892990.
E-mail address: j.e.tenelshof@utwente.nl (J.E. ten Elshof).

0021-9797/$ - see front matter © 2010 Elsevier Inc. All rights reserved.
doi:10.1016/j.jcis.2010.12.011

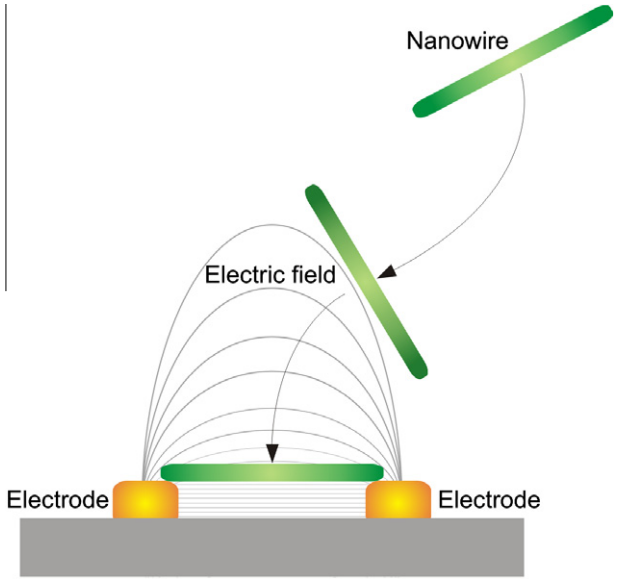

Fig. 1. Schematic representation of dielectrophoretic alignment of nanowires between two parallel plate electrodes.

medium, negative dielectrophoresis will occur and the nanowires will drift away from the electrodes. The same principle holds for dielectrophoretic alignment of nanotubes.

Quite different solvent media, peak-to-peak potentials, frequencies, and electrode gaps have been used for the dielectrophoretic alignment of various types of nanowire materials. An overview of reported parameters in the literature is listed in Table 1. The variation in the data suggests that the parameters may not have been chosen systematically, although they led to successful alignment in all cases. Only one paper systematically addresses the influence of frequency [27], and only one paper could be found in which the influence of the applied potential was systematically investigated [28]. The influence on the adhesion between nanowires and substrate, viscosity, and vapor pressure were noted as reasons to choose specific solvents [19,21].

The goal of the research presented here is to determine the ranges in which these parameters lead to successful alignment of nanowires and nanotubes of varying composition. From this information, a universal set of parameters for dielectrophoretic alignment of metal and metal oxide nanowires and nanotubes of arbitrary composition is derived. The parameters that we investigated are peak-to-peak potential and frequency, thickness of the insulating silicon oxide layer, grounding of the silicon substrate, and the medium used. We chose to investigate water and dichloromethane as solvents, since these are members of two opposite classes of liquids, namely polar high-permittivity, and nonpolar low-permittivity media, respectively. Furthermore, the nanowires are already dispersed in dichloromethane after the track-etched polycarbonate template has been dissolved.

Table 2
Material properties used for the calculations of Fig. 4.

Material property	Au	Fe_2O_3	H_2O	CH_2Cl_2
$\varepsilon/\varepsilon_0$[a]	Infinite	12 [33]	78.32 [33]	8.93 [33]
σ (S/m)	4.5×10^9 [27]	1×10^{-12} [34]	1×10^{-4} [27]	0.8×10^{-4} [35]
κ (m^{-1})			2.0×10^7	1.27×10^9
η (Pa s)			8.90×10^{-4} [33]	4.13×10^{-4} [33]

[a] ε_0 is the permittivity of vacuum (8.85419×10^{-12} F/m).

2. Experimental details

All chemicals used were obtained from commercial sources and used without further purification. Silver nitrate ($AgNO_3$) and nitric acid (HNO_3, 65%) were purchased from Acros Organics. Chloroauric acid trihydrate ($HAuCl_4{\cdot}3H_2O$), nickel sulfate hexahydrate ($NiSO_4{\cdot}6H_2O$), boric acid (H_3BO_3), zinc nitrate hexahydrate ($Zn(NO_3)_2{\cdot}6H_2O$), iron nitrate nonahydrate ($Fe(NO_3)_3{\cdot}9H_2O$), sodium hydroxide (NaOH), indium, and dichloromethane (CH_2Cl_2) were purchased from Merck. Buffered hydrofluoric acid (BHF; HF and NH_4F) was purchased from BASF. Milli-Q water with a resistivity of 18.2 MΩ cm was used in all experiments.

Nanowires and nanotubes were made by templated electrodeposition in a conventional three-electrode setup. First a gold layer was sputtered onto a polycarbonate track-etched membrane (Whatman, UK) using a Perkin-Elmer 2400 sputtering system. The Au layer (also called back electrode) was used as working electrode in the electrochemical deposition process. Prior to deposition, the backside of the back electrode was isolated to ensure exclusive deposition inside the pores of the membrane and avoid deposition on the external surface of the back electrode. A small Pt mesh was used as counter electrode and Ag/AgCl in 3 M KCl (REF 321 from Radiometer Analytical) was used as reference electrode. The electrodes were connected to a potentiostat (Bank Electronik Potentioscan Wenking POS 73) linked to two multimeters (a Keithley 197 Autoranging microvolt DMM multimeter and a Peaktech 4385 multimeter with a USB port for automatic data collection). For electrodeposition of nanowires, the electrodes were placed inside a plating solution. The corresponding recipes are described below. After the membrane pores were completely filled by deposited material, or when a segment with the desired length had been

Table 1
Overview of parameters reported in literature for dielectrophoretic alignment of nanowires.

Nanowire material	Medium	Potential (V)	Frequency (kHz)	Electrode gap (μm)	Electric field (V/μm)	Refs.
Au	Methanol	0.97	150	2	0.485	[16]
Au	Methanol	10	>100	2	5	[16]
Au-biotin	Methanol	0.18	1000	2	0.09	[16]
ZnO	Ethanol	5	1000	6–10	0.833–0.5	[17]
ZnO	Ethanol	5	1000	4	1.25	[18]
Ag	Ethanol	0.1	5	4	0.025	[18]
Ag or Au	H_2O or EtOH	0.2	100	±30	±0.00667	[19]
Rh rods	Acetone	10	Unknown	5–30	2–0.333	[20]
CNT[a]	Acetone	45	Unknown	5–30	9–1.5	[20]
p-Si	Benzyl alcohol	110	10	40	2.75	[21]
Si	IPA[b] and H_2O	0.35	0.5	2	0.175	[28]

[a] CNT, carbon nanotube.
[b] IPA, isopropanol.

obtained, deposition was stopped by removing the potential. Then the membrane was rinsed with Milli-Q water. In the final steps, the nanowires or nanotubes were collected by first dissolving the polycarbonate membrane in CH_2Cl_2, followed by detaching them from the Au back electrode by gentle swirling.

Gold nanowires were formed from an electrolyte containing 0.005 M $HAuCl_4{\cdot}3H_2O$. Deposition occurred either at a constant potential of +0.25 V or at a saw-tooth potential oscillating between +0.97 and 0 V with a linear rate of 10 mV/s. Ni nanowires were formed from an electrolyte containing 0.23 M $NiSO_4{\cdot}6H_2O$ and 0.15 M H_3BO_3. Deposition occurred at −1.00 V. The deposition conditions for Ag and ZnO nanowires and Fe_2O_3 nanotubes have been explained elsewhere [12]. In short, Ag nanowires were formed at +0.10 V in an electrolyte containing 0.20 M $AgNO_3$ and 0.10 M H_3BO_3 with pH adjusted to 1.5 using HNO_3. ZnO nanowires were formed at 70 °C at −1.00 V in an electrolyte containing 0.10 M $Zn(NO_3)_2{\cdot}6H_2O$. The iron hydroxide gel was formed using an electrolyte containing 0.02 M $Fe(NO_3)_3{\cdot}9H_2O$, 0.430 M HNO_3, and 0.425 M NaOH. Gel formation occurred at −1.00 V and the nanotubes formed upon drying. Sn nanowires were formed from an electrolyte solution containing 0.01 M $SnCl_2$ and a few drops of HCl. Deposition occurred at −0.55 V. Axially segmented nanowires were prepared by alternating deposition of the desired materials using the above-described procedure, and rinsing with Milli-Q water of the membrane, reference electrode, and platinum mesh.

The nanowires and nanotubes were aligned using dielectrophoresis on prepatterned silicon wafers (LioniX, Enschede, The Netherlands). The prepatterned Au microelectrodes were completely embedded in the native silicon oxide layer. Before the experiments, a 300 nm thick layer of native oxide was etched away to elevate the Au surface approximately 75 nm above the surrounding oxide surface. After placing the patterned wafer in a buffered hydrofluoric acid solution (BHF; containing HF and NH_4F) (DANGER! HF—the active component of BHF—is a very dangerous chemical that causes severe burns and bone loss without immediately producing pain, so extra care needs to be taken!) for the required amount of time (78 nm/min), the substrates were washed several times with Milli-Q water.

Fig. 2 is a schematic representation of the dielectrophoresis setup. A similar setup was previously used by Gierhart et al. [27] and Ahmed et al. [29]. A sinusoidal AC voltage was applied between the Au electrodes using a sweep generator (Wavetek 11 MHz stabilized sweep generator Model 22). The potential was measured using an oscilloscope (Hameg Instruments 35 MHz analog oscilloscope HM 303-6). Both sweep generator and oscilloscope were connected to an amplifier (Techron 7570 power supply amplifier). A resistance R_1 of 14.5 kΩ was added in series to limit the current flowing through aligned nanowires. A resistance R_2 of 9.5 kΩ was added in parallel to prevent the potential across the electrodes from being sensitive to impedance changes in the solution during nanowire alignment. The Au microelectrodes were connected to an external circuit using Cu wires connected to the microelectrodes using indium contacts. The dielectrophoresis experiments consisted of placing a droplet of nanowire solution on top of the electrodes while applying an AC voltage at typical frequencies of 50–200 kHz. In a typical dielectrophoresis experiment, the measured potential on the oscilloscope dropped within a few seconds to a few minutes to almost zero, indicating successful alignment of the nanowires.

Scanning electron microscopy (SEM) images were taken using a Zeiss HR-LEO 1550 FEF SEM. *IV* curves were measured using a CV measurements Karl Suss PM8 low-leakage manual probe station connected to a Keithley 4200 semiconductor characterization system with PreAmps, PGU/OSC and CVU.

3. Results and discussion

Fig. 3 shows SEM images of several nanowires after deposition onto a silicon wafer. When ferromagnetic nanowires or nanowires with a high surface energy were formed, such as Ni or ZnO, they typically clustered once the membrane had been dissolved. The clustered nanowires could be redispersed by ultrasonication. The inset of this figure shows a typical example of an isolated nickel nanowire after ultrasonication. Isolated nanowires were observed in the case of Au, Ag, and Sn nanowires, and in the case of Fe_2O_3 nanotubes. The synthesized wires had a length of 4–6 μm and a diameter of 50–150 nm. The length depends on the electrodeposition time and the variation in diameter over the length of the wire is due to the shape of the polycarbonate membrane pores. The diameter near the entrance of the pores is 50 nm and measures 150 nm in the center.

3.1. Dielectrophoretic alignment

The initial experiments identified four parameters that are crucial for proper alignment of nanowires and nanotubes. These are peak-to-peak potential and frequency, thickness of the silicon oxide layer, grounding of the silicon substrate, and the solvent medium used. These parameters will be discussed in more detail in the following subsections.

3.1.1. Peak-to-peak potential and frequency

The potential used in dielectrophoretic alignment can be chosen arbitrarily as it only defines the strength of the generated

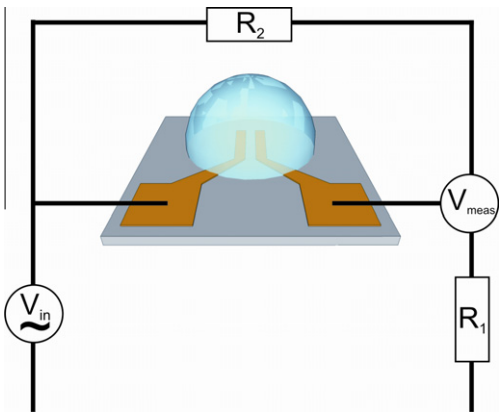

Fig. 2. Instrumentation circuit for dielectrophoretic nanowire capture with R_1 = 14.5 kΩ and R_2 = 9.5 kΩ.

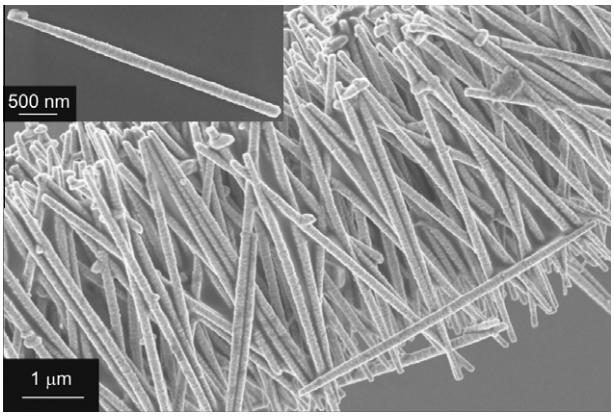

Fig. 3. SEM images of a cluster of Ni nanowires. Inset: a single Ni nanowire showing the variation in diameter.

dielectrophoretic force; the higher the applied potential, the higher the force. We chose to apply potentials that are sufficiently low to prevent noticeable decomposition of H_2O, the most easily decomposable solvent used in this study. A sinusoidal alternating current with a peak-to-peak potential V_0 of 2.1 V results in an effective potential of 1.5 V in the case of a DC potential or in the case of an AC potential with a low frequency. This is only just above the theoretical decomposition potential of H_2O (1.4 V) and well below its practical decomposition potential of 2.0 V. For AC potentials with higher frequencies, this decomposition potential will be higher, and therefore no chemical reactions or gas evolution occurred in any of the dielectrophoretic alignment experiments.

The frequency dependence of dielectrophoretic alignment follows from the equation for dielectrophoretic force (Eq. (1)) and the equation for electroosmotic fluid velocity (Eq. (7)). The need for the dielectric constant of the nanowires to be higher than the dielectric constant of the surrounding medium is expressed in Eq. (1) for spherical particles [27].

$$\vec{F} \propto \varepsilon_m \mathrm{Re}\left(\frac{\varepsilon_p^* - \varepsilon_m^*}{\varepsilon_p^* + 2\varepsilon_m^*}\right) \vec{\nabla} |\vec{E}|^2, \tag{1}$$

where $\vec{F}$ is the dielectrophoretic force, ε_m is the dielectric constant of the solvent medium, $\mathrm{Re}\left(\frac{\varepsilon_p^* - \varepsilon_m^*}{\varepsilon_p^* + 2\varepsilon_m^*}\right)$ is the real part of the Clausius–Mossotti factor $\left(\frac{\varepsilon_p^* - \varepsilon_m^*}{\varepsilon_p^* + 2\varepsilon_m^*}\right)$, ε_m^* is the complex dielectric constant of the solvent medium, ε_p^* is the complex dielectric constant of the particle and $\vec{E}$ is the external electric field. The complex dielectric constants ε_m^* and ε_p^* can be calculated from

$$\varepsilon_k^* = \varepsilon_k - \frac{j\sigma_k}{\omega}, \tag{2}$$

where ε_k is the real part of the dielectric constant in which k can be either p or m for particles or solvent medium, respectively, j is the square root of -1, σ_k the electrical conductivity of the nanowire material or solvent, and ω the angular frequency of the applied electric field. For nanorods and nanowires, a shape-dependent factor A_α is introduced into the Clausius–Mossotti factor [29],

$$K_\alpha = \left(\frac{\varepsilon_p^* - \varepsilon_m^*}{\left(\varepsilon_p^* - \varepsilon_m^*\right)A_\alpha + \varepsilon_m^*}\right), \tag{3}$$

where K_α is the shape-dependent Clausius–Mossotti factor, in which the index α can either refer to L for the long axis of the nanowire or to S for its short axis, and where A_α is the depolarization factor along the long or short axis of a prolate ellipsoid.

$$A_L = \frac{1-e^2}{2e^3}\left[\ln\left(\frac{1+e}{1-e}\right) - 2e\right] \tag{4}$$

and

$$A_S = \frac{(1-A_L)}{2}, \tag{5}$$

where e is defined as the eccentricity:

$$e^2 = 1 - \frac{b^2}{a^2}. \tag{6}$$

Here a and b are the half length of the long axis and the radius of the short axis, respectively [29].

Eq. (7) gives the fluid velocity $\langle v \rangle$ near the electrode surface [27]. The fluid velocity is directed away from the center of the electrode gap, and is induced by AC electroosmosis. AC electroosmosis occurs at symmetric, coplanar microelectrode gaps such as those used in this study.

$$\langle v \rangle = \frac{1}{8}\frac{\varepsilon_m V_0^2 \Omega^2}{\eta x (1+\Omega^2)^2}, \tag{7}$$

where V_0 is the peak-to-peak potential, Ω is the dimensionless frequency which is defined by Eq. (8), η is the viscosity of the solvent, and x is the distance from the center of the electrode gap to one of the electrodes.

$$\Omega = \omega x \frac{\varepsilon_m}{\sigma_m}\frac{\pi}{2}\kappa, \tag{8}$$

where κ is the inverse of the Debye–Hückel length [27], which can be calculated by

$$\kappa = \sqrt{\frac{q^2 \sum n_i^0 z_i^2}{\varepsilon_m k T}}, \tag{9}$$

where q is the elementary charge 1.6×10^{-19} C, n_i^0 and z_i are the number concentration and ionic charge of the ionic species type i present in solution, respectively, k is Boltzmann's constant (1.381×10^{-23} J/K), and T is the temperature.

Fig. 4a and b show the calculated AC electroosmotic fluid velocities $\langle v \rangle$ of nanowires with a diameter of 150 nm as a function of the field frequency in H_2O and CH_2Cl_2, respectively. Data from Table 2 were used in the calculations. Fluid flow is absent at both low and high frequencies. At high frequencies, the velocity is small because the charged ions in solution are not fast enough to follow the rapidly changing polarities of the electrodes. However, very low frequencies are also unsuitable, so only frequencies beyond the frequency range for electroosmotic fluid flow in H_2O or CH_2Cl_2 are applicable. Following the results from the models presented in Fig. 4a and b, frequencies above 10^4 and 10^3 Hz should be used for H_2O and CH_2Cl_2, respectively.

However, when the real part of the Clausius–Mossotti factor, Eq. (3), is also taken into account, it follows that the suitable frequency for nonmetallic nanowires and nanotubes should be at least 10^5 Hz when they are dispersed in dichloromethane; see Fig. 4f. If nonmetallic nanowires or nanotubes are dispersed in water, only negative dielectrophoresis was observed as shown in Fig. 4e. For metallic nanowires with a theoretically infinite permittivity, no such restriction applies; see Fig. 4c and d. The green areas in Fig. 4 mark the universally suitable frequency ranges for dielectrophoresis. As frequencies beyond 10^8 Hz are not commonly used and hard to apply, a frequency of $1.2–2.0 \times 10^5$ Hz was adopted in all further dielectrophoretic alignment experiments.

3.1.2. Influence of the substrate

We observed that the silicon substrate underneath the silicon oxide layer became electrostatically charged when the SiO_2 layer of the substrate was too thin. The charging resulted in a positive electric field gradient in the middle of the electrode gap and away from the electrode gap in the vertical direction that prevented the nanowires from aligning in between the smallest electrode gap [29]. Fig. 5 shows the simulated electric field and electric field gradients in the vicinity of the electrodes for three given thicknesses of the insulating silicon oxide layer. These simulations were obtained from FlexPDE using a distance between the electrodes of 2.5 μm in all three cases. As the electrodes were embedded for 400 nm in the native SiO_2 layer, an overall SiO_2 layer thickness of 1 μm yielded an effectively 600 nm thick insulating layer between the Si bulk and the Au electrodes. In this case, the underlying Si substrate was charged by electrostatics, as shown in Fig. 5a. This resulted in a countercharge that gives rise to an electrostatic force directed away from the Au electrodes, thereby disrupting the possibility of proper alignment. The simulations suggest that the energetically most favorable position for a nanowire is in a floating position just above the electrodes. This hampers their alignment and ability to connect with the electrodes.

With a SiO_2 layer of 2.5 μm thickness (providing an effective thickness of 2.1 μm), no attractive or repulsive forces act in the middle of the electrode gap, as indicated by the red curve in

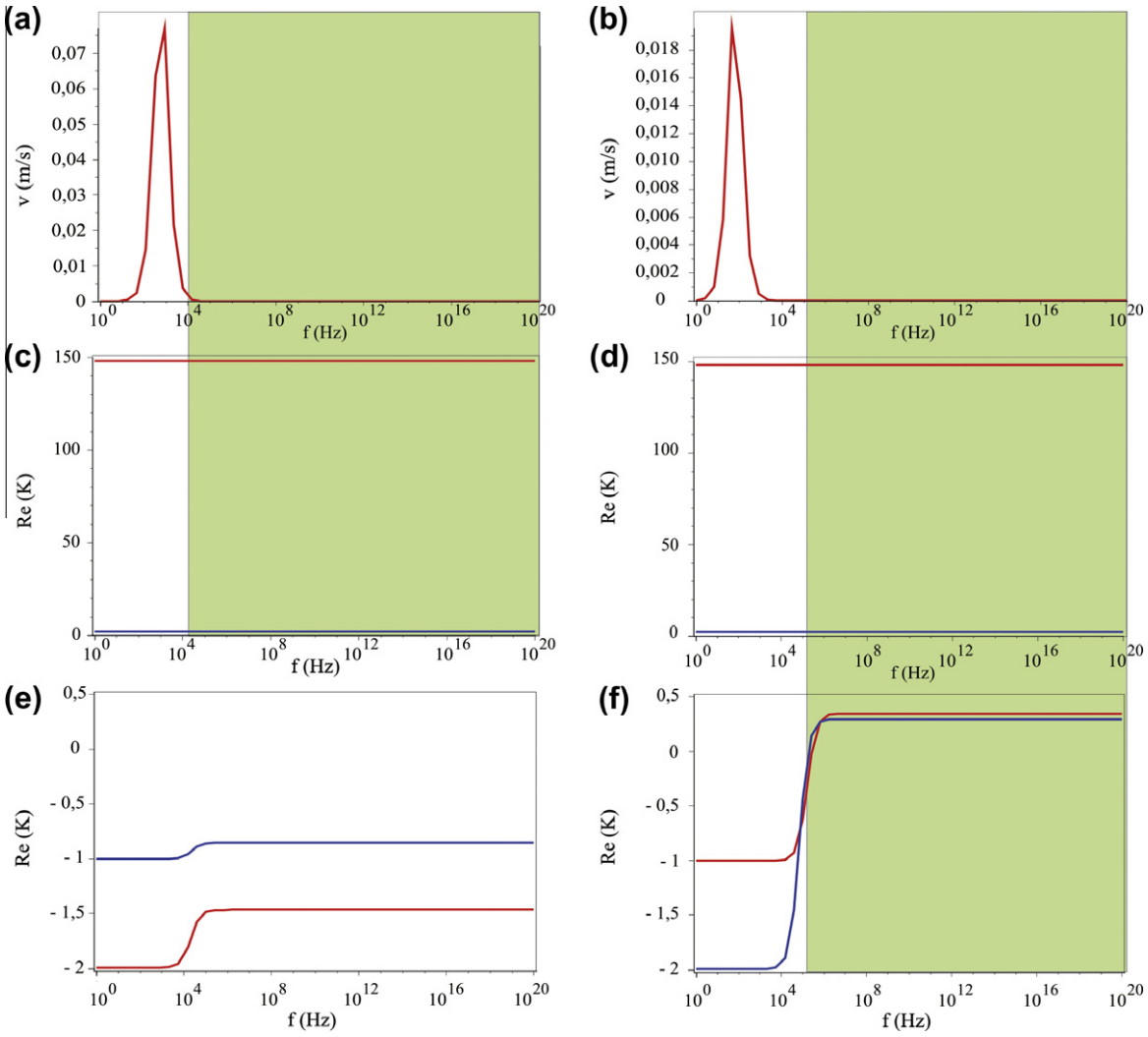

Fig. 4. (a and b) Calculated electroosmotic fluid velocity of nanowires in H_2O and CH_2Cl_2, respectively. The real part of the Clausius–Mossotti factor is shown in (c–f) for a number of cases: (c) Au nanowires in H_2O; (d) Au nanowires in CH_2Cl_2; (e) Fe_2O_3 nanotubes in H_2O; and (f) Fe_2O_3 nanotubes in CH_2Cl_2. The red curves in (c–f) represent the real parts of the Clausius–Mossotti factor along the short axis of the nanowires or nanotubes, and the blue curves represent the same factor along the long axis. The relevant material properties of Au, Fe_2O_3, H_2O, and CH_2Cl_2 used to construct these graphs are listed in Table 2. T = 298 K, x = 1.25 μm. and V_0 = 2.1 V was used. (For interpretation of the references to colour in this figure legend, the reader is referred to the web version of this article.)

Fig. 5d. This is the minimum oxide layer thickness required for proper alignment. The repulsive forces acting in the middle of the electrode gap are close to zero, and a net attractive force results from the areas closer to the Au electrode. Fig. 5c and the blue curve in Fig. 5d show the situation in the case of an 8 μm thick silicon oxide layer (providing an effective thickness of 7.6 μm). The electric field gradient promotes proper positioning and alignment of nanowires from any position and orientation in the liquid phase.

3.1.3. Grounding of the silicon substrate

In addition to having a sufficiently thick oxide layer, grounding of the substrate was also found to be of crucial importance. In the electric field simulations in Fig. 5, the potential of the silicon substrate was set to 0 V. Because the potential of the silicon substrate will be floating if the silicon substrate is not grounded, the alignment process would be negatively influenced. Once the silicon substrate was grounded, positive alignment was observed as can be seen in Fig. 6.

3.1.4. Solvent medium

The fourth parameter is the medium used. According to Eq. (1), the dielectric constant of the nanowire should be higher than the dielectric constant of the medium in order to exert an effectively attractive force on the wire. The use of CH_2Cl_2 or H_2O as the solvent will not influence the alignment of metal nanowires with an infinite permittivity such as Au, Ni, Ag, and Sn, whereas CH_2Cl_2 ($\varepsilon/\varepsilon_0 = 8.93$) is the preferred solvent for the alignment of metal oxide nanowires and nanotubes such as ZnO ($\varepsilon/\varepsilon_0 = 8.15$) and Fe_2O_3 ($\varepsilon/\varepsilon_0 = 12$).

Interestingly, while the dielectric constant of undoped ZnO is a little smaller than that of CH_2Cl_2 and negative dielectrophoresis is therefore expected, we were still able to align ZnO nanowires. This is illustrated in Fig. 6b. The most likely reason to explain this observation is that the dielectric constant of the nanowires is actually higher than that of pure ZnO. It has been reported that the dielectric constant of *n*-type doped ZnO is higher than that of pure ZnO. For instance, a dielectric constant of 15.1 has been reported by Dhananjay et al. for 15 mol.% lithium-doped ZnO thin films [30]. In a similar manner, it is possible that the dielectric constant of the ZnO nanowires in the present study is higher than that of CH_2Cl_2 due to the presence of low concentrations of impurities or structural defects, e.g., vacancies, grain boundaries, and/or surface defects, and that would explain the positive dielectrophoresis effect that we observed.

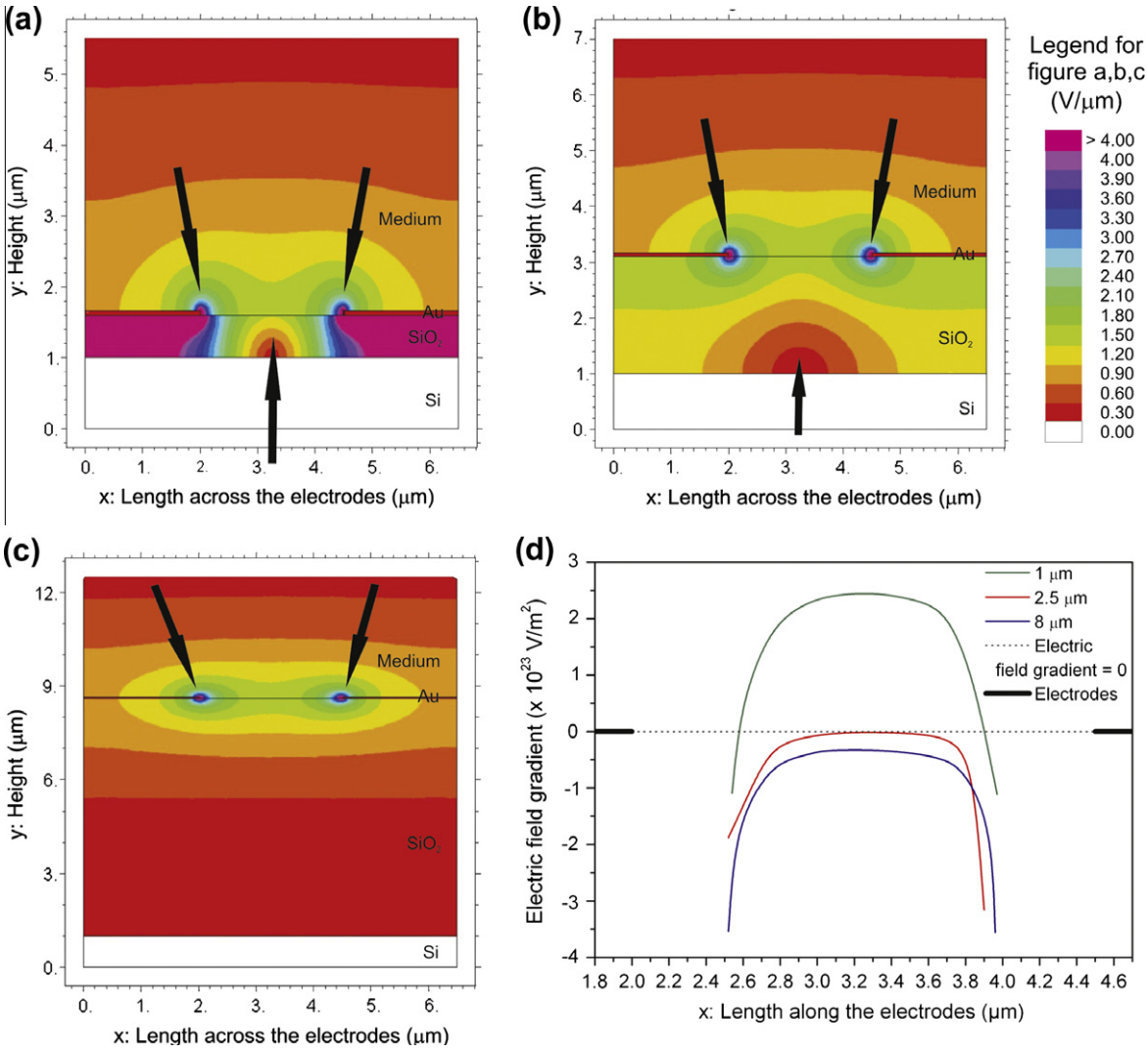

Fig. 5. (a–c) Simulated local electric fields $E(x, y)$ in the vicinity of the electrodes and (d) electric field gradients $dE(x, y)/dy$ in between the electrodes; (a) and green curve in (d), silicon oxide layer thickness of 1 μm; (b) and red curve in (d), silicon oxide layer thickness of 2.5 μm; (c) and blue curve in (d), silicon oxide layer thickness of 8 μm. The arrows in (a–c) indicate the direction and strength of the attractive and repulsive forces at the position of the arrow tip. (For interpretation of the references to colour in this figure legend, the reader is referred to the web version of this article.)

3.1.5. Combination of the dielectrophoretic alignment parameters

A universal set of parameters can be defined that is based on the combined results of the above-described experiments. It involves applying a field with a frequency $>10^5$ Hz, an insulating silicon oxide layer with a thickness of 2.5 μm or more, grounding of the underlying silicon substrate, and the use of a solvent medium with a low dielectric constant. In our experiments, we obtained good results by using a peak-to-peak potential of 2.1 V at a frequency of 1.2×10^5 Hz. Fig. 6 shows an overview of nanowires and nanotubes of various compositions after alignment using these parameters. Although not every experiment led to successful alignment after applying only one droplet, perfect alignment was observed at almost every sample after applying the second or the third droplet. Especially Fe_2O_3 nanotubes, either filled with Ni or not, were found to align with a reproducibility of 100%.

The coaxial Fe_2O_3–Ni nanowire shown in Fig. 6e was molten onto the electrodes at both ends. As the electrical contact area between the coaxial nanowire and the electrodes is increased, we called this "nanosoldering" of nanowires or nanotubes onto the electrodes. As Fe_2O_3 is an insulating material, it was not possible to measure an increased current from this sample, but we believe that nanosoldering could improve the electrical contact between nanowires or nanotubes and the electrodes. Nanosoldering is accomplished by melting of the nanowires and/or parts of the Au electrodes close to the wire due to the high current through the nanowire that is generated as soon as physical contact is made with both electrodes. When the nanowire material is highly conductive and has a relatively low melting point, as in the case of Ag, Au, or Sn, the complete nanowire can actually melt immediately after alignment, and we observed this phenomenon in a number of cases. To prevent burning of the nanowires, an indirect alignment technique is proposed below. Using this indirect alignment technique, nanowires or nanotubes could be aligned without short circuiting after alignment.

3.2. Indirect alignment of nanowires

A schematic representation of the proposed technique is shown in Fig. 7. The idea behind the indirect alignment technique is that the distance between the potentiostatically charged electrodes 1 and 3 is so large that any leakage current will flow primarily via the floating electrode 0. As electrode 0 is not connected to the

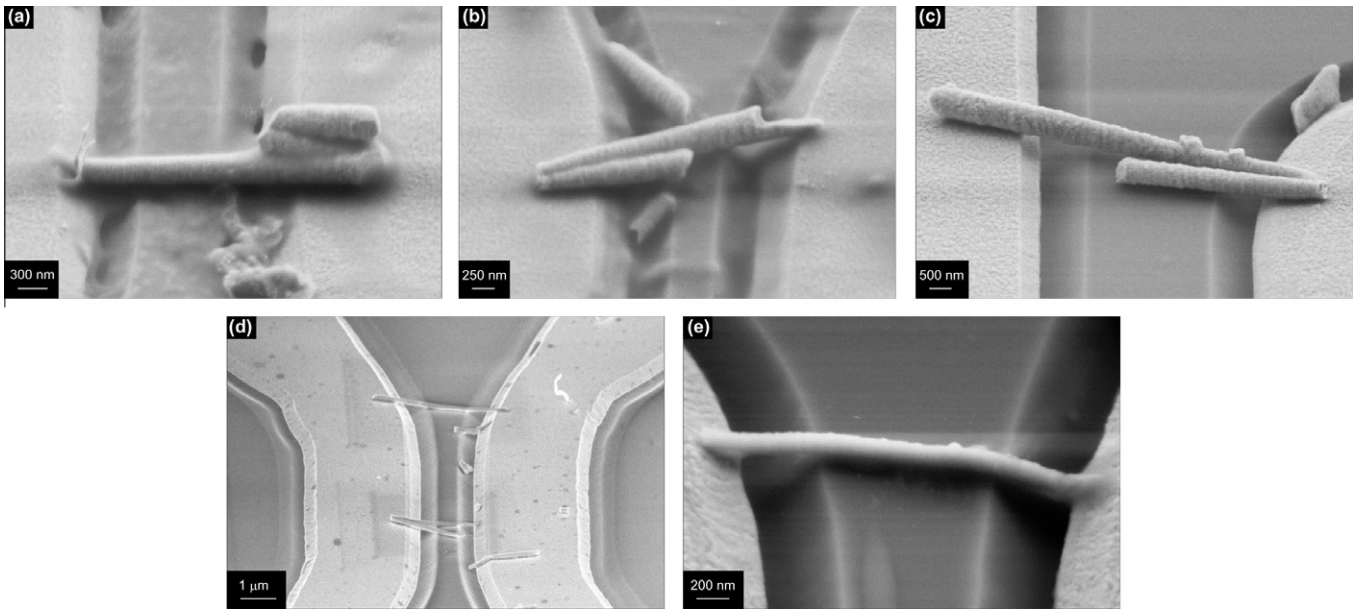

Fig. 6. SEM images of a dielectrophoretically aligned (a) Ag nanowire, (b) ZnO nanowire, (c) segmented Ag|ZnO nanowire, (d) Fe_2O_3 nanotube, and (e) coaxial Fe_2O_3–Ni nanowire.

potential generator, no significant current flows through it. However, since a small electrical field is present between 0 and its counterelectrodes that is strong enough to orient and align the nanowires, effective dielectrophoretic alignment without risk of short circuiting was accomplished. After indirect alignment experiments, nanowires could not only be found between electrode 0 and electrodes 1 and 3, but also between electrode 0 and electrode 2.

Fig. 8 shows SEM images of some examples of nanowires and nanotubes aligned by using the indirect alignment technique. Applied peak-to-peak potentials were in the range of 0.6–6 V. Such high peak-to-peak potentials were possible in this case because CH_2Cl_2 was used as solvent medium, which has a higher decomposition potential than water.

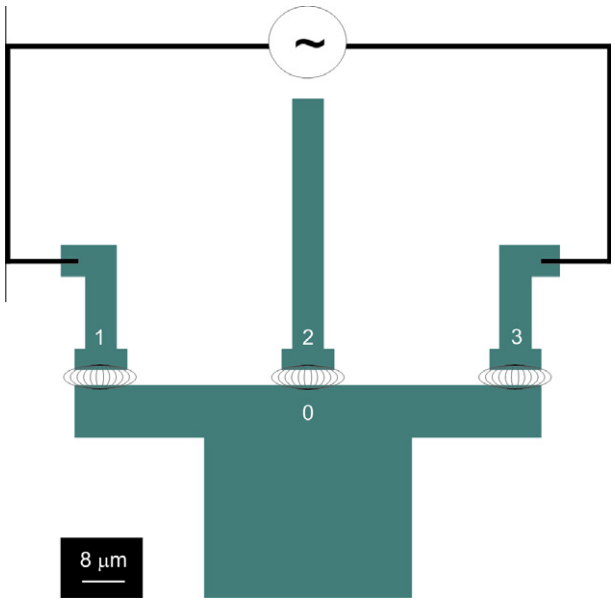

Fig. 7. Schematic representation of the indirect alignment technique; electrodes 0 and 2 are floating. Local fields will develop between 1 and 0, between 3 and 0, and between 2 and 0.

3.3. Resistivity measurements

Fig. 9 shows the *IV* curve of the ZnO nanowire shown in Fig. 6b. From the dimensions of the nanowire, a resistivity of 2.2–3.4 × 10^{-3} Ωm was estimated. This is considerably lower than the values obtained by Postels et al. [31] and Heo et al. [32] for ZnO nanorods

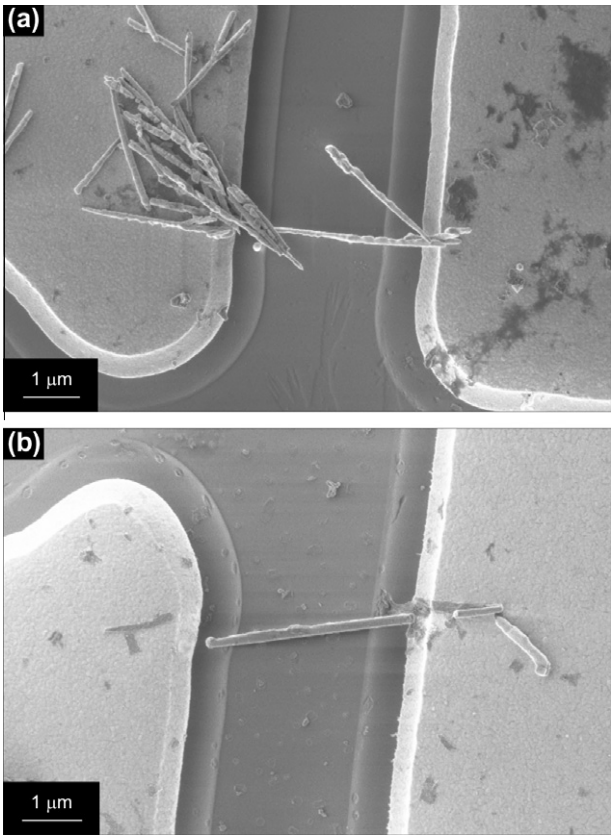

Fig. 8. Top-view SEM image of (a) Au and (b) Sn nanowires aligned by the indirect alignment technique.

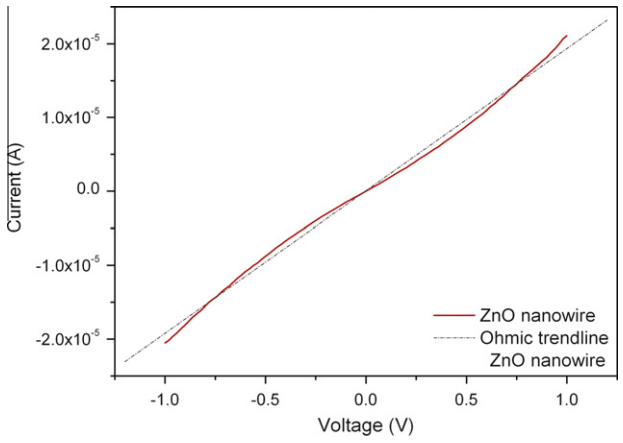

Fig. 9. *IV* curve of a ZnO nanowire after alignment by dielectrophoresis.

made by electrochemical deposition (10 Ωm) and molecular beam epitaxy (MBE) (500 Ωm), respectively. The high conductivity is in qualitative agreement with the observed positive dielectrophoresis, as it suggests the presence of a substantial concentration of defects that would explain the high conductivity.

4. Conclusions

The dielectrophoretic alignment of metallic and oxidic nanowires between coplanar electrodes is primarily determined by four parameters. These parameters are: (1) a peak-to-peak potential below the decomposition potential of the solvent medium used at a frequency higher than 10^5 Hz, (2) a silicon oxide layer with a minimum thickness of 2.5 μm, (3) grounding of the silicon substrate underneath the silicon oxide layer, and (4) the use of CH_2Cl_2 or other organic solvent with a low dielectric constant as solvent medium. An indirect alignment technique was proposed to prevent short circuiting of the nanowires after alignment. After alignment, a considerably lower resistivity was found for ZnO nanowires made by templated electrodeposition compared to ZnO nanorods synthesized by electrodeposition or molecular beam epitaxy.

Acknowledgments

Financial support from the Dutch Ministry of Economic Affairs in the framework of the NanoNed programme is acknowledged. One of the authors (W.A.) acknowledges support from the Higher Education Commission in Pakistan.

References

[1] Y.W. Heo, D.P. Norton, L.C. Tien, Y. Kwon, B.S. Kang, F. Ren, S.J. Pearton, J.R. Laroche, Mater. Sci. Eng. R: Rep. 47 (2004) 1.
[2] R. Fan, R. Karnik, M. Yue, D. Li, A. Majumdar, P. Yang, Nano Lett. 5 (2005) 1633.
[3] F. Patolsky, G. Zheng, C.M. Lieber, Anal. Chem. 78 (2006) 4260.
[4] C.D. Keating, M.J. Natan, Adv. Mater. 15 (2003) 451.
[5] L.A. Bauer, D.H. Reich, G.J. Meyer, Langmuir 19 (2003) 7043.
[6] J. Wang, J. Mater. Chem. 18 (2008) 4017.
[7] W.F. Paxton, S. Sundararajan, T.E. Mallouk, A. Sen, Angew. Chem. Int. Ed. 45 (2006) 5420.
[8] Y. Wang, R.M. Hernandez, D.J. Bartlett Jr, J.M. Bingham, T.R. Kline, A. Sen, T.E. Mallouk, Langmuir 22 (2006) 10451.
[9] J. Wang, ACS Nano 3 (2009) 4.
[10] Y. Rheem, C.M. Hangarter, E.H. Yang, D.Y. Park, N.V. Myung, B. Yoo, IEEE Trans. Nanotechnol. 7 (2008) 251.
[11] S.J. Hurst, E.K. Payne, L. Qin, C.A. Mirkin, Angew. Chem. Int. Ed. 45 (2006) 2672.
[12] M.G. Maas, E.J.B. Rodijk, W. Maijenburg, J.E. ten Elshof, D.H. A. Blank, Multifunction at the Nanoscale through Nanowires, 2010, 1206-M01-08.
[13] M. Meyyappan, M. Sunkara, Inorganic Nanowires: Applications, Properties, and Characterization, Boca Raton, FL, 2010.
[14] R.M. Langford, T.X. Wang, M. Thornton, A. Heidelberg, J.G. Sheridan, W. Blau, R. Leahy, J. Vac. Sci. Technol. B 24 (2006) 2306.
[15] G. De Marzi, D. Lacopino, A.J. Quinn, G. Redmond, J. Appl. Phys. 96 (2004) 3458.
[16] J.J. Boote, S.D. Evans, Nanotechnology 16 (2005) 1500.
[17] A. Yoon, W.K. Hong, T. Lee, J. Nanosci. Nanotechnol. 7 (2007) 4101.
[18] C.S. Lao, J. Liu, P. Gao, L. Zhang, D. Davidovic, R. Tummala, Z.L. Wang, Nano Lett. 6 (2006) 263.
[19] S.J. Papadakis, Z. Gu, D.H. Gracias, Appl. Phys. Lett. 88 (2006).
[20] S. Evoy, N. DiLello, V. Deshpande, A. Narayanan, H. Liu, M. Riegelman, B.R. Martin, B. Hailer, J.C. Bradley, W. Weiss, T.S. Mayer, Y. Gogotsi, H.H. Bau, T.E. Mallouk, S. Raman, Microelectron. Eng. 75 (2004) 31.
[21] A.D. Wissner-Gross, Nanotechnology 17 (2006) 4986.
[22] C.M. Hangarter, N.V. Myung, Chem. Mater. 17 (2005) 1320.
[23] L. Clime, T. Veres, J. Colloid Interface Sci. 326 (2008) 511.
[24] M. Tanase, L.A. Bauer, A. Hultgren, D.M. Silevitch, L. Sun, D.H. Reich, P.C. Searson, G.J. Meyer, Nano Lett. 1 (2001) 155.
[25] M. Tanase, D.M. Silevitch, A. Hultgren, L.A. Bauer, P.C. Searson, G.J. Meyer, D.H. Reich, J. Appl. Phys. 91 (2002) 8549.
[26] D.H. Reich, M. Tanase, A. Hultgren, L.A. Bauer, C.S. Chen, G.J. Meyer, J. Appl. Phys. 93 (2003) 7275.
[27] B.C. Gierhart, D.G. Howitt, S.J. Chen, R.L. Smith, S.D. Collins, Langmuir 23 (2007) 12450.
[28] E.M. Freer, O. Grachev, D.P. Stumbo, Nat. Nanotech. 5 (2010) 525.
[29] W. Ahmed, E.S. Kooij, A. Van Silfhout, B. Poelsema, Nano Lett. 9 (2009) 3786.
[30] Dhananjay, S. Singh, J. Nagaraju, S.B. Krupanidhi, Appl. Phys. A 88 (2007) 421.
[31] B. Postels, A. Bakin, H.H. Wehmann, M. Suleiman, T. Weimann, P. Hinze, A. Waag, Appl. Phys. A 91 (2008) 595.
[32] Y.W. Heo, L.C. Tien, D.P. Norton, B.S. Kang, F. Ren, B.P. Gila, S.J. Pearton, Appl. Phys. Lett. 85 (2004) 2002.
[33] D.R. Lide, CRC Handbook of Chemistry and Physics, CRC Press, Boca Raton, FL, 2010.
[34] F. Morin, Bell Syst. Technol. J. 37 (1958) 1047.
[35] G. Lindsten, Electrically Conductive Fluids, US5104582, 1992.